Porous ceramic bodies for drug delivery

A. KRAJEWSKI, A. RAVAGLIOLI, E. RONCARI, P. PINASCO
Institute for Technological Research on Ceramics - C.N.R., Faenza, Italy
L. MONTANARI
Interdisciplinary Clinical and Pharmacological Group, Faenza, Italy
E-mail: kraxi@irtec1.irtec.bo.cnr.it

An approach to the production of ceramic drug delivery devices is proposed. Two examples of possible ceramics are dealt with: hydroxyapatite weakly modifiable by living tissue and the bioinert alumina. The possibility to control the formed porosity was taken into consideration for both materials. The ratio between the acquired porosity and the quantity and quality of the agents inducing porosity is also described and discussed. A test on the role of porosity was performed on the obtained porous ceramic bodies and a study was made on the release of a substance with pharmacological activity from previously impregnated porous ceramic bodies. This paper is preliminary to a planned work targeted to the preparation of ceramic drug delivery systems.

1. Introduction

The traditional methods of supplying substances at pharmacological activity to patients is the instantaneous intake through injection or oral ingestion. Instantaneous absorption permeates the whole living body, and indiscriminate diffusion and absorption of the supplied substances involves all tissues, healthy and seriously ill.

The development of delivery systems was a necessary scientific attempt to solve the problem of supplying the active principles only where they are needed by a slow, local, continuous and controled flux (over days, months or years).

Apart from the diseased tissue, the protagonists of this new supplying method are the type of substance and the porosity of the delivering surface. Between these two protagonists there are possible correlations.

The flux of a substance across a porous layer is connected to two main parameters: its solubility in the interested solution (in this case the physiological liquids) and the possible physical or chemical bonds formed by its molecules with the walls of the pores of the delivery device. The porous layer, which comes into contact with the living tissues, must have a chemical and physical nature biocompatible with the surrounding living tissues. Moreover, its microstructure must be compatible with its target, which is the functional activity of flux regulation of delivering; in particular its pore size distribution must ensure a continuous controlled release over time for a functional use of the dispenser. Some attempts were also made by the authors [1–5] to simulate the solution adopted by Mother Nature.

The target of the activity described here was: (1) to study a suitable porous microstructure enabling to release the pharmacological substances over easily predictable times by a computation with a suitable flow rate as required by medical needs; (2) to prepare devices of suitable size and geometric shape (depending on medical requirements), warranting manufacturing repeatability.

There are many pharmacological substances (antibiotic, anticancer, anti-phlogistic, and also hormones, insulin, steroids, etc.) which can be delivered by these porous devices. The chemical nature of the ceramic can also be changed to better correspond to the chemical characteristics of these substances. A compound like $Ca_5(PO_4)_3OH$ (hydroxyapatite), code HA, was considered to be used to prepare possible resorbable delivery devices, while Al_2O_3 (Alumina), code AL, was instead considered to be used when a re-extraction has to be planned.

To solve this problem, particular emphasis was given to the nature of the pore structure. It will be decisive to understand the mechanism of drug movement from ceramics through the formed porous architecture. Apart from biocompatibility, the microstructure of the ceramic must guarantee functional flux regulation of delivery; in particular, its pore size distribution must warrant a continuous controlled release over time to program the functional use of the dispenser.

2. Materials and methods

2.1. Preparation of porous ceramic bodies

Commercial powders of AL (Reynolds) and HA medical grade (Riedel de Haën), with an average particle diameter of 0.32 μm and 0.35 μm respectively were used as starting materials. The specific surface area of AL powder, measured by the single point BET method (Sorpty 1750, Carlo Erba, Milano) is $7\ m^2g^{-1}$. To reduce the packing volume and improve the mixing step of the extrusion process, HA powders were previously calcined at 900 °C for 1 h. The heat treatment decreases the specific surface area of the HA powders from 61 to

$5\,m^2g^{-1}$ and increases the mean particle diameter from 0.35 to 0.89 μm. Polyvinyl-butirrale (PVB) (B-76 Monsanto Co.) and carbon fibers (diameter 7 μm, length < 3 mm; CFT3, DuPont De Nemours Co.), coded B and C respectively, were utilized as porosity inducing agents (PIAs). Selected PIAs were utilized either alone or together in suitable mixture ratios. Different ratios of PIAs and ceramic powder were tested to produce samples with different size distribution and pore morphology. The ceramic powder is dry homogenized for 1 h in a planetary mixer with a plasticizer (Zusoplast PS-1) and the wanted amount of PIAs (PVB). At the same time the binder is cold dissolved in a separate beaker with the least amount of distilled water. The binder solution is then added to the homogenized powders together with some more water and all is mixed for a further 2 h. Once the mixture has formed, carbon fibers are eventually added by a further mixing process (1 h).

Different formulations of starting composition to be extruded were obtained for both AL and HA ceramics as reported in Table I. Samples A1 (for AL) and H1 (for HA) were made to compare the type and amount of porosity obtained by thermal treatment of extruded samples without addition of PIAs.

Each mixture was then estruded at 25 MPa through a 10 mm diameter extrusion hole. The extruded samples were dried at room temperature in a special box starting from an initial relative humidity greater than 70%. The AL and HA samples were sintered at 1300 °C and 1170 °C respectively, with a soaking time of 1 h.

The heat treatment was defined on the basis of thermogravimetric investigations. PVB burns out completely in the 300 °C–500 °C range while carbon fibers exhibit a far slower decomposition process which starts at 200 °C and ends at 720 °C. In both cases the process is exothermal. The sintering thermal cycle was therefore planned with a first slow heating rate (50 °C/h) until 600 °C to favor a good decomposition and elimination of the organic materials (binders, plasticizers and PIAs). Above 600 °C a second step (100 °C/h) was planned until the wanted sintering temperature was reached.

After sintering, cylindrical samples with diameter 9.5 ($\pm$ 0.3) mm and height 14.3 ($\pm$ 0.3) mm (mean volume = $1020 \pm 100\,mm^3$) were accurately cut by a diamond wheel to have samples with the same dimensions; the volume V of the samples is reported in Tables II and III.

Porosity of the sintered samples was measured by mercury porosimeter (Mod. 2000, Carlo Erba, Milano) and examined by scanning electron microscope (SEM) (Cambridge Stereoscan 360). The obtained porosities were gathered in 5 porosimetric intervals of pore radius. These were slightly differently adapted for alumina and HA samples. The values coming from the porosimeter are listed in a column of relative porosity (RP%); from these values, taking into account the porosity of the sample (in practice the overall volume of mercury threaded into the ceramic body referred to the volume of the sample), was calculated the absolute porosity (AP%) listed in another column; a third column reports the volumetric porosity (VP) as the amount of porosity referred to the sample volume.

2.2. Impregnation with a drug and release test

Both AL and HA cylindrical samples were impregnated with a methanol solution of hydrocortisone acetate (HCA) (lot n. 950004, Polichimica *Snc*., Bologna) at a concentration of $3.5\,mg\,ml^{-1}$. Each cylinder was imbibed with 0.6 ml of such solution for a total amount of 2.1 mg of HCA. The adopted pharmacological substance, commonly used as antiphlogistic steroid, is insoluble in water ($0.01\,mg\,ml^{-1}$) but highly soluble in methanol ($3.9\,mg\,ml^{-1}$). Every sample was left 24 h in sterilised air (37 °C), and then put into 100 ml of a saline solution of NaCl 0.9% in bi-distilled water (''*physiological solution*'', Eurospital SpA, Trieste) for the release test. The beakers containing the samples with the solution were kept continuously shaking through a waving oscillating device to allow dispersion of the released molecules in the solution, without formation of liquid layers with concentration gradient. Absorbency

TABLE I Formulations of alumina (AL) and hydroxyapatite (HA) mixtures

	Alumina sample composition (wt %)						
	A1	AB1	AB2	AC1	AC2	ABC1	ABC2
Alumina	77.54	73.64	65.88	80.87	76.80	72.57	65.06
Binder and plasticizer	0.74	0.59	0.53	0.56	0.53	1.60	1.43
Water	21.71	18.41	20.42	17.90	18.82	20.32	23.10
Carbon fibers (C)	–	–	–	0.67	3.84	2.03	3.90
PVB (B)	–	7.36	13.18	–	–	3.48	6.51
	Hydroxyapatite sample composition (wt %)						
	H1	HB1	HB2	HC1	HC2	HBC1	HBC2
Hydroxyapatite	63.42	55.80	56.28	58.41	55.49	57.40	54.29
Binder and plasticizer	1.19	1.23	0.39	1.29	1.22	1.14	1.20
Water	35.39	37.39	33.77	39.14	40.51	36.50	35.29
Carbon fibers (C)	–	–	–	1.17	2.77	1.83	3.26
PVB (B)	–	5.58	9.57	–	–	3.13	5.97

TABLE II Porosimetric characteristics of the alumina samples

	A1			AB1			AB2			AC1			AC2			ABC1			ABC2		
$V \pm \Delta V$ (mm^3)	1022 ± 16			1018 ± 20			1020 ± 10			1024 ± 18			859 ± 8			1020 ± 10			803 ± 15		
Porosity (%)	20.18			34.20			42.55			23.56			27.67			29.09			40.21		
Pore radius (μm)	RP (%)	AP (%)	VP (mm^3)	RP (%)	AP (%)	VP (mm^3)	RP (%)	AP (%)	VP (mm^3)	RP (%)	AP (%)	VP (mm^3)	RP (%)	AP (%)	VP (mm^3)	RP (%)	AP (%)	VP (mm^3)	RP (%)	AP (%)	VP (cm^3)
(1)* <0.01	0.00	–	–	0.00	–	–	0.00	–	–	0.00	–	–	0.00	–	–	0.00	–	–	0.00	–	–
(1)* 0.01 ÷ 0.10	99.27	20.03	204.7	59.93	20.49	208.6	33.06	14.07	143.5	92.46	21.78	223.0	84.37	23.34	200.5	63.62	18.51	188.8	33.02	13.28	106.6
(2)* 0.10 ÷ 0.50	0.00	–	–	14.14	4.84	49.3	7.72	3.28	33.5	0	–	–	8.67	2.40	20.6	17.23	5.01	51.1	3.40	1.38	11.1
(3)* 0.50 ÷ 1.50	0.00	–	–	17.50	5.99	61.0	31.06	13.22	134.8	3.38	0.80	8.1	3.98	1.10	9.5	10.24	2.98	30.4	8.73	3.50	28.2
(4)* >1.50	0.73	0.15	1.5	8.43	2.88	29.3	28.16	11.98	122.2	4.16	0.98	10.0	2.98	0.83	7.1	8.91	2.59	26.4	54.85	22.05	177.1
Total	100	20.18	206.2	100	34.20	348.2	100	42.55	434.0	100	23.56	241.1	100	27.67	237.7	100	29.09	296.7	100	40.21	323.0

V = volume of the cylindrical sample; $\pm \Delta V$ = volume standard deviation; RP = relative porosity (volume % of each porosimetric class on all porosity volume); AP = absolute porosity (% of the porosity referred to the sample volume); VP = Volumetric porosity (volume of the porosity); (*) porosity class number, the same number correspond to the pedices of the coefficient ''a'' of the WMSP analysis.

TABLE III Porosimetric characteristics of the hydroxyapatite samples

	H1			HB1			HB2			HC1			HC2			HBC1			HBC2		
$V \pm \Delta V$ (mm^3)	1022 ± 20			1024 ± 20			1018 ± 21			1020 ± 18			1020 ± 20			1021 ± 20			1015 ± 19		
Porosity (%)	40.54			44.50			46.16			46.49			37.60			39.56			40.29		
Pore radius (μm)	RP (%)	AP (%)	VP (mm^3)	RP (%)	AP (%)	VP (mm^3)	RP (%)	AP (%)	VP (mm^3)	RP (%)	AP (%)	VP (mm^3)	RP (%)	AP (%)	VP (mm^3)	RP (%)	AP (%)	VP (mm^3)	RP (%)	AP (%)	VP (cm^3)
(1)* <0.01	0.50	0.20	0.0	1.5	0.67	10.0	0.00	–	–	0.00	–	–	0.31	0.11	–	0.00	–	–	0.00	–	–
(1)* 0.01÷0.10	3.75	1.52	10.0	2.84	1.26	10.0	4.50	2.08	20.0	6.95	3.23	30.0	4.77	1.79	20.0	1.97	0.78	10.0	2.63	1.06	10.0
(2)* 0.10÷0.50	94.29	38.23	390.0	90.33	40.20	410.0	81.27	37.51	380.0	85.01	39.52	40.0	79.17	29.77	300.0	73.51	29.08	300.0	61.76	24.88	250.0
(3)* 0.50÷1.50	0.34	0.14	0.0	3.59	1.59	10.0	10.13	4.68	50.0	1.83	0.85	10.0	7.30	2.74	30.0	6.08	2.41	20.0	4.59	1.85	20.0
(4)* >1.50	1.11	0.45	10.0	1.77	0.78	10.0	4.09	1.89	20.0	6.18	2.87	30.0	8.48	3.19	30.0	18.45	7.29	70.0	31.03	12.50	130.0
Total	100	40.54	410.0	100	44.50	450.0	100	46.16	470.0	100	46.47	470.0	100	37.60	380.0	100	39.56	390.0	100	40.29	410.0

V = volume of the cylindrical sample; $\pm\Delta V$ = volume standard deviation; RP = relative porosity (volume % of each porosimetric class on all porosity volume); AP = absolute porosity (% of the porosity referred to the sample volume); VP = Volumetric porosity (volume of the porosity); (*) porosity class number, the same number correspond to the pedices of the coefficient ''a'' of the WMSP analysis.

measurements were performed on each solution through a spectrophotometer (Perkin-Elmer mod. 55B) at regular intervals, to follow the release of the pharmacological substance in time. The wavelength of measurement, on which the phenanthrene group of HCA molecule is activated, was 242 nm. The test was carried out making reference to a curve drawn by measuring the intensity of absorbency of a standard solutions containing known concentrations of HCA. In all cases the measurements were placed in the linearity range of the calibration curve.

2.3. Mathematical elaborations

To evaluate a correlation between sample porosity and drug release a simple diffusional model was chosen to try to obtain useful parametric values for a comparison between different porous samples based on the following equation:

$$ln\mathrm{y} = ln\left(\frac{C_1(0) - C_2(t)}{C_1(0) - C_2(0)}\right) = ln\kappa + mt$$

where $C_1(0)$ is drug concentration inside the porous sample at time 0; $C_2(0)$ is drug concentration in the solution surrounding the sample at time 0; $C_2(t)$ is drug concentration in the solution surrounding the sample at a time $t>0$. For the experimental boundary conditions adopted in the experiment $C_2(0) = 0$. The terms $ln\kappa$ and m on the right are constants. The reported equation corresponds to a straight line in a plot lny towards t in which $ln\kappa$ represents the intercept on the lny axis for the time $t = 0$ and m the slope of the line. Different values of $ln\kappa$ and m were obtained from every sample. Those pertaining to alumina are listed in Table IV, whereas those pertaining to hydroxyapatite in Table V.

For more information the different pore size distribution of alumina and hydroxyapatite samples was divided in four classes indicated with Arabian numbers in Tables II and III. To evaluate the specific contribution of the different classes of porosity to the release rate a system of linear relationship was used expressed by an equation like: $\Sigma_i a_i r_i = m$, where m is the flow rate coefficient previously found and r_i and a_i are respectively the pore radius (the mean value of the range of every class) and the correspondent coefficient of proportionality. The pedices i are extended from 1 to 4, referred to the specific class of Tables II and III. A best fitting was carried out on the equations system through a standard weighed mean square procedure (WMSP) yielding the values of a_i for alumina and hydroxyapatite ceramics.

3. Results

The samples porosity as a function of the PIAs concentration is reported in Fig. 1. The comparison displays a very different behavior of the two materials. In particular AL ceramic is sensible to the PIAs presence, showing a linear relationship between porosity and their addition, apart from the nature of added PIAs. HA, on the contrary, shows a random distribution statistically contained in a horizontal band centered along the straight-line having equation ''Porosity %'' = 42.2.

3.1. Alumina porous ceramics

3.1.1. Porosity

As reported in Table I, the maximum concentration of PIAs type B was 13.18 wt % (samples AB2) whereas it was impossible to overcome the value of 3.84 wt % with PIAs type C (samples AC2). When both B and C PIAs are added together, the amount of PVB is slightly higher than the amount of C fibers, with the B/C ratio of 1.71 and 1.67 for the ABC1 and ABC2 respectively. The quantity of binder and plasticizers is low and restricted in the range of $0.5 \div 0.7$ wt % for all samples having only one PIAs, a value which increases when both B and C PIAs have to be added together. Table II reports the porosity of all AL samples subdivided in significative intervals. This value is also presented as volume % compared to the overall one of the cylinder. The whole porosity of sample

TABLE IV Equation coefficients coming from equation $ln(y) = lnk + mt$ for alumina samples

Sample	ln k	m ($\times 10^{-3}$)	R^2
A1	− 0.30	− 7.602	0.970
AB1	− 0.32	− 1.905	0.796
AB2	− 0.30	− 7.602	0.970
AC1	− 0.55	− 11.528	0.970
AC2	− 0.18	− 2.926	0.997
ABC1	− 0.37	− 2.679	0.818
ABC	− 0.27	− 3.177	0.987

TABLE V Equation coefficients coming from equation $ln(y) = lnk + mt$ for hydroxyapatite samples

Sample	ln k	m ($\times 10^{-3}$)	R^2
H1	− 0.093	− 4.900	0.997
HB1	− 0.074	− 5.431	0.999
HB2	− 0.074	− 5.431	0.999
HC1	− 0.074	− 5.445	0.998
HC2	− 0.074	− 5.453	0.998
HBC1	− 0.075	− 5.468	0.997
HBC	− 0.075	− 5.473	0.998

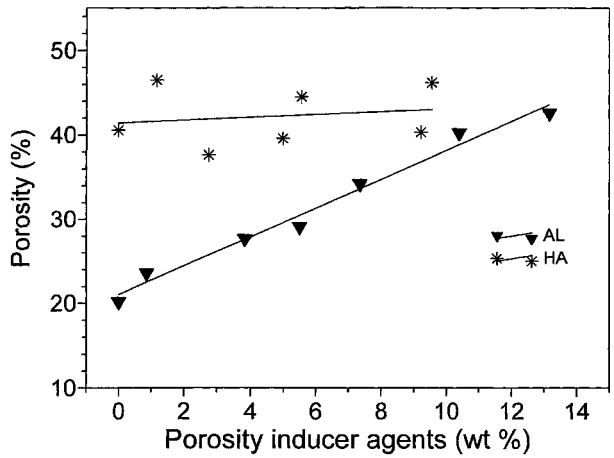

Figure 1 Porosity (%) of alumina and HA samples as a function of porosity inducing agents (PIAs) concentration (wt %).

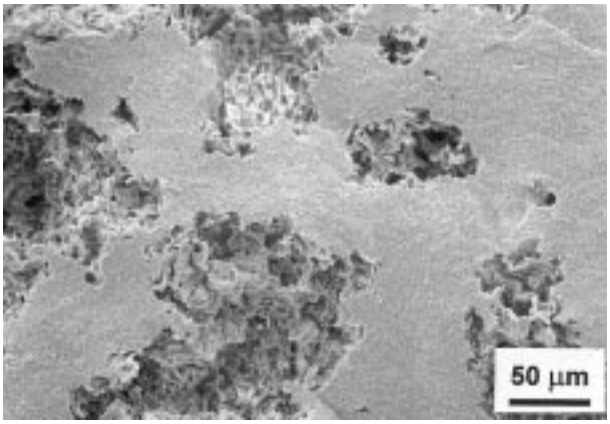

Figure 3 SEM micrograph of cross section fracture of sample AB2 (1300 °C, 1 h).

A1 (20.18%) is essentially formed of small size pores in a very close range of $0.01 \div 0.10\,\mu m$ (average diameter 0.07 μm). It exhibits by SEM investigation an homogeneous microstructure with roundish grains (Fig. 2) according to the observed monomodal pore distribution (grain diameter ranging from 0.1 and 0.5 μm). Porosity comes from the spaces left free between the grains that were bound together after sintering, forming a three-dimensional porous structure. Such a micro-porosity may be considered ''*structural*'' and therefore present in all AL sintered samples at 1300 °C. From Table II it is possible to observe that the addition of PIAs determines a decrease of the finest structural porosity $(0.01 \div 0.10\,\mu m)$ in favor of other classes of pores, whose amount and dimension are connected to the nature and amount of employed PIAs. An addition of B PIEs drastically increases the porosity until 42.55% (AB2). The porosity distribution becomes bimodal, with a lower structural microporosity but with new intermediate porosity centerd at 0.8 μm and 1.5 μm for AB1 and AB2 respectively. This meso-porosity is induced exclusively by the presence of B PIEs. Cross sections of the samples observed by SEM reveal that PVB, after its complete destruction, leaves an irregularly shaped porosity with diameter sizes of up to 100 μm (Fig. 3). This fraction of large holes, not revealed by porosimetric analysis, is interconnected only through pores of far lower diameter, included in the $1 \div 10\,\mu m$ interval. In practice these large holes represent a kind of special internal reservoir that can be accessed only through holes of diameter not greater than 10 μm. The addition of carbon fibers increases the porosity to a maximum value of 28% (AC2) with a little decrease of ''structural'' porosity. This is a consequence both of the smaller amount of PIEs employed (3.84 wt % of carbon fibers in sample AC2 compared with 13.18 wt % of PVB in sample AB2) and of the different morphology.

The simultaneous recourse to PVB and carbon fibers together causes the formation of a structure in which both globular and thread-like pores are present, as shown in the surface SEM analysis of the fracture normal to extrusion flow of sample ABC1 (Fig. 4); it is evident that the fibers have a tendency to displace parallel to the flow direction of the extrusion. It is also possible that a portion of the pores that come from the decomposition of carbon fibers communicates with the pores that come from the decomposition of PVB, giving rise to a variously articulated porosity network. When both B and C PIEs occur at high concentration (ABC2), the presence of pores with diameter higher than 1.5 μm becomes relevant.

3.1.2. Release

The curves of increasing concentration of the released HCA in time coming from the different alumina ceramic samples are reported in Fig. 5. The variation of the

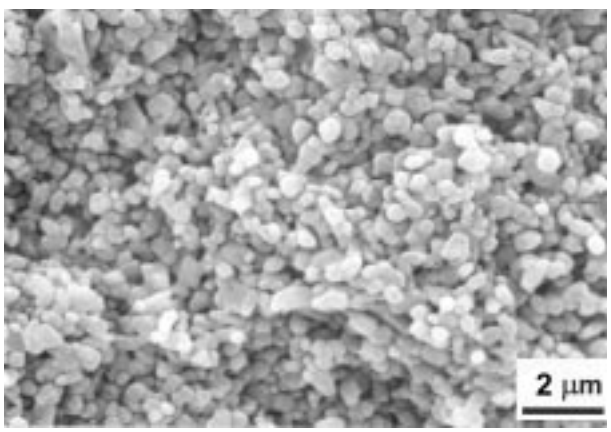

Figure 2 SEM micrograph of cross section fracture of sample A1 (1300 °C, 1 h).

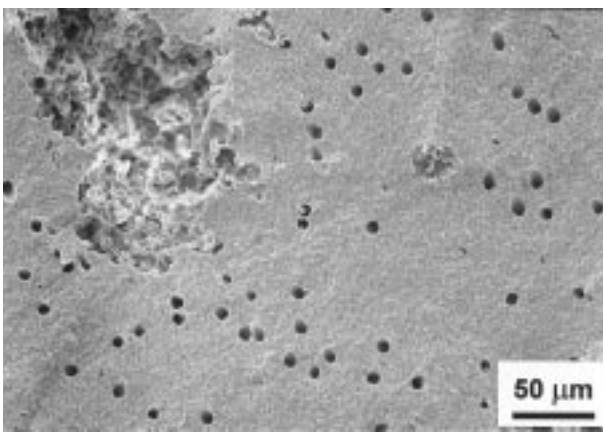

Figure 4 SEM micrograph of cross section fracture of sample ABC1 (1300 °C, 1 h).

obtained values ranges in an interval of $\pm$ 5%. These curves indicates that an influence on the release speed is connected with the porosity.

Using the drug concentration value at different time reported in Fig. 5 and the formula mentioned in section 2.3, we obtained by mathematical elaboration a straight line (Fig. 6) for every different alumina sample, whose slope m is reported in Table IV.

The WMPS elaboration on these m values of each sample towards the correspondent VP ones (expressed in cm^3) coming from every porosity class has supplied: $a_1 = -3.2$, $a_2 = 0.2$, $a_3 = 0.0$, $a_4 = -1.2$ (standard error = 1.5).

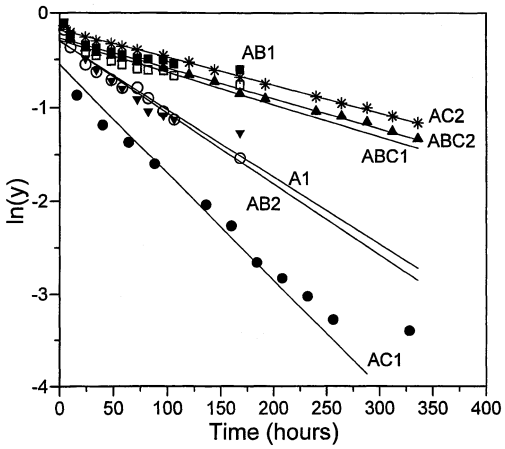

Figure 6 Release of HCA from alumina samples following the equation reported in section 2.3.

3.2. HA porous ceramics

3.2.1. Material

For all HA compositions (Table I) a higher quantity of water (about 35%) is necessary in respect to AL formulation. This greater amount of water is due more to the physico-chemical characteristics of HA powders (greater specific surface area, greater hydrophilicity, etc.) than to the need of solubilising the organic additives employed in no higher concentration than those for alumina. On the other hand it was not possible to overcome a maximum amount of 10 wt % of B PIAs, while this value did not overcome 2.77 wt % when C PIAs was used.

The intervals of porosity, reported in Table III, show that for HA ceramic a microstructure is obtained whose porosity lies prevalently in the $0.25 \div 0.50$ μm range. This structural porosity is higher than that formed in the correspondent extruded alumina samples. H1 samples exhibit a monomodal pore distribution with grain diameters ranging from 0.3 μm to 0.7 μm. Altogether, if the different bulk morphology in respect to that of alumina is not considered, the addition of PVB induces the formation of irregularly shaped pores, giving rise to a situation similar to that seen for the samples with alumina. The percent of structural porosity decreases with the increase of added PIAs until a minimum of 61% for HBC2 samples. The decrease of the percent of this porosimetric interval brings about an increase of larger pores (for a mean amount of about 2/3) and a formation of narrower pores (for a mean amount of about 1/3). Not unlike in the correspondent alumina samples, in this case too there is a sensible occurrence of macroporosity, with values that may overcome 30%. Differently from alumina samples, however, the whole porosity remains quite constant. Total porosity does not increase with the increase of the concentration of PIAs by using either PVB or carbonium fibers or both of them. This apparently anomalous behavior may be due to a different arrangement of the fibers inside the body, an arrangement difficult to control. With B PIAs there also occur big holes of about 100 μm, while the introduction of carbonium fibers (HC samples) brings to the formation of long pores. If these pores are longitudinally opened they appear as long furrows in a homogeneous microstructure equal to that of H1. They exhibit a 10 μm diameter and a 300 μm length and are displaced parallel to the flow direction of the extrusion, as shown by a SEM investigation on cross sections parallel to the cylindric principal axis (Fig. 7).

3.2.2. Release

The curves of increasing concentration of the HCA released in time from the different HA ceramic samples are reported in Fig. 8. The obtained values vary in an interval of $\pm$ 5%. In this case it is very hard to establish

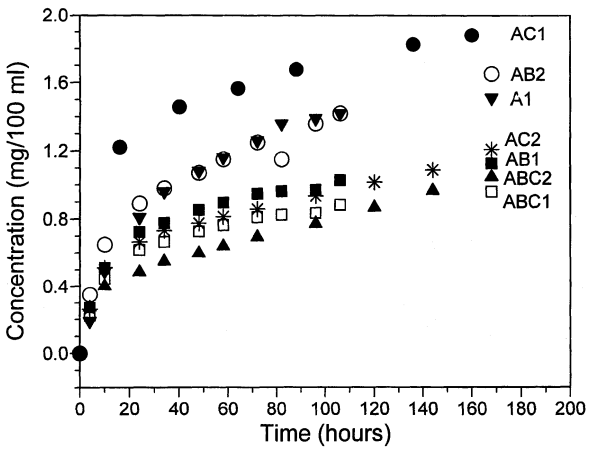

Figure 5 Release trend of HCA from alumina samples.

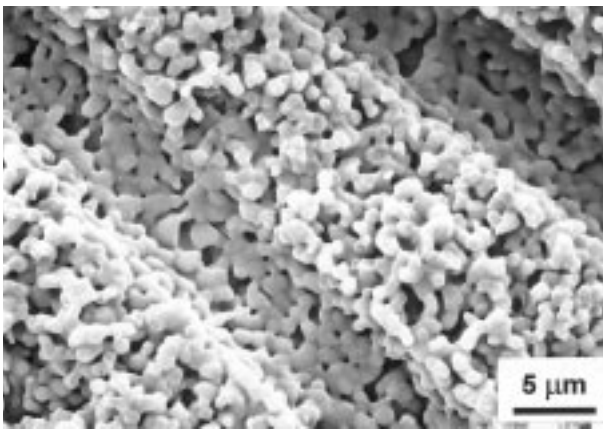

Figure 7 SEM micrograph of cross section parallel to the axis of extrusion of a sample HC2 (1170 °C, 1 h).

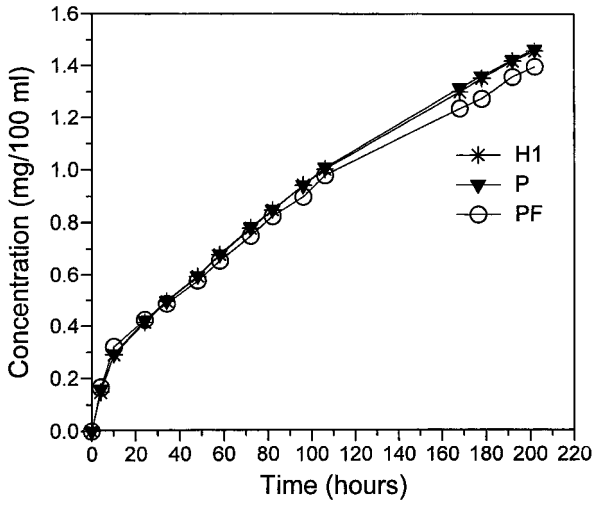

Figure 8 Release trend of HCA from indicated HA samples. H1 = HA without PIAs; P = all samples treated with PVB; PF = all samples containing fibers (with or without PVB).

if an influence on the release speed is connected with the porosity, being all the curve superposed.

Using the drug concentration value at different time reported in Fig. 8 and the formula mentioned in section 2.3 and adopting the same procedure followed for alumina samples we obtained a straight line (Fig. 9) whose slope m is reported in Table V.

The WMPS elaboration on these m values of each sample towards the correspondent VP values (expressed in cm^3) coming from every porosity class supplied: $a_1 = -3.9$, $a_2 = -1.2$, $a_3 = -1.6$, $a_4 = -1.7$ (standard error = 3.8) with the only significant value of a_1.

4. Discussion

The addition of PIAs produces a general percent increase of larger porosity on both alumina and hydroxyapatite materials. In particular PIAs addition has no practical effects on the total porosity of HA ceramic (practically the same VP porosity), although there is a redistribution of the percent amount of the different intervals of porosity. This is attributed to the wide overcoming of the threshold limit of the intergranular neck shrinkage. On the other hand, a firing at lower temperatures of the samples prepared in the indicated way does not supply a sufficiently consolidated porous ceramic material. In practice HA ceramic sintered at 1170 °C is in the phase of intergranular porosity contraction regulated by wet angle among grains. It was ergo observed that the reasonable constancy of the whole porosity is followed by a substantial constancy of the flux release rate of HCA. At a first sight this might be interpreted as a consequence, but a proportional relationship between total porosity and release flux seems to be excluded on the basis of the results coming from alumina samples. On the contrary, in fact, the quantity and dimension of pores are connected to the kind of PIAs utilized for Al_2O_3 ceramic with firing at 1300 °C, which proved to be a very interesting material for drug delivery devices. On the other hand, the observed releases appear to grant a sufficiently durable release in time (at least *in vitro*). Obviously, to reach a very durable release a recourse to a porous capsule becomes necessary (a porous shell including a wide cavity as reservoir to be filled with the substance). However, PIAs addition brings about a decrease in finest porosity, with formation of pores of wider dimensions. It is obvious that the flow through the porous wall is connected to the amount of pharmacological substance, the viscosity of the liquid, the number of open pores inside the body and at the surface, their diameter, shape, length and tortuosity. All these parameters must obey the Bernoulli's fluid dynamic equation applied to irrotational incompressible flow. Every kind of tortuosity introduces a pressure load lost during the flow. In our case, imbibition resulted in the filling of the finest pores (as expected according to Lord Kelvin's theory for wet substances).

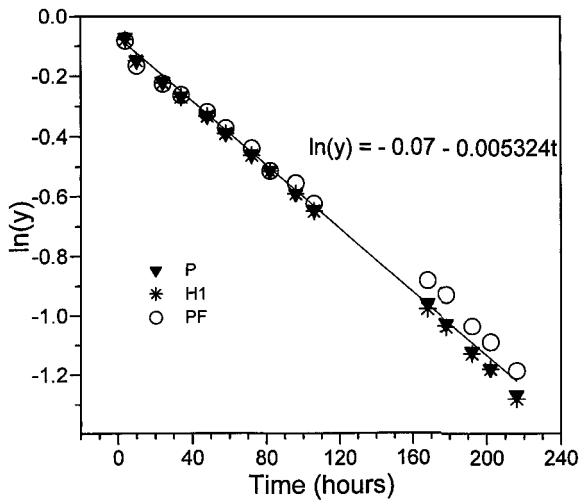

Figure 9 Release of HCA from hydroxyapatite samples following the equation reported in Section 2.3.

5. Conclusions

This study allowed a plausible interpretation of the phenomena involved in releasing a substance with pharmacological activity and simple molecular structure from ceramic samples with different porosimetric intervals, preventively impregnated with that substance. The acquired experiences suggest the adoption of releasing devices with porous walls with pores as fine as possible in order to produce delivery systems able to grant long times of low level and possibly always constant release.

The interpretation of data, however, suggests different roles in the dimensional distribution of the different pores. Pores of greater size drive the pharmacological molecules out of the porous body by a diffusion movement across the solvent, which remains stationary in these pores; in the meantime the finest pores slowly absorb solvent from the solution surrounding the porous body, which gradually fills the volume let free from the fraction of the pharmacological substance as it dissolves and/or leaves the interior of the porous body. This leads to suppose that particular dimensional distributions of pores could exist, with different degrees of efficiency in the release

mechanism: some of these are particularly efficient, while other are even not able to move the process of diffusion and stall. This conclusion privileges a bimodal rather than a monomodal dimensional distribution of porosity, also pointing out the better combinations of size and amount of the two classes of pores.

References

1. W. J. BUYKX, *J. Australian Ceram. Soc*. **29**(1/2) (1993) 23–31.
2. R. MARTINETTI, H. DENISSEN, E. RONCARI, P. PINASCO and C. MANGANO, in ''Fourth EuroCeramics–Vol. 8'', Edited by A. Ravaglioli (Faenza Editrice, Faenza, Italy, 1995) pp. 53–60.
3. H. DENISSEN, E. VAN BEEK, R. MARTINETTI, C. KLEIN, E. VAN DER ZEE and A. RAVAGLIOLI, *J. Period. Res*. **32** (1997) 40–46.
4. A. RAVAGLIOLI, A. KRAJEWSKI, I. PANTIERI and G. SCARPA, *Ceramica Acta* **10**(2–3) (1998) 17–30.
5. A. KRAJEWSKI, A. RAVAGLIOLI, E. RONCARI, P. PINASCO, L. MONTANARI and I. PANTIERI, in ''Bioceramics'', Vol. 11, edited by R. Z. LeGeros and J. P. LeGeros (World Scientific Publ. Co. Pte. Ltd., New York, 1998) pp. 533–536.

Received 8 December 1999
and accepted 30 March 2000